SUPPLEMENTARY INFORMATION

Tunable Thermal Bioswitches for *In Vivo* Control of Microbial Therapeutics

Dan I. Piraner[1, 2, #], Mohamad H. Abedi[2, #], Brittany A. Moser[1], Audrey Lee-Gosselin[1], Mikhail G. Shapiro[1, *]

[1]Division of Chemistry and Chemical Engineering,

[2]Division of Biology and Biological Engineering

California Institute of Technology

Pasadena, CA, USA 91125

[#]Equal contribution

*Correspondence should be addressed to MGS:

Email: mikhail@caltech.edu

Nature Chemical Biology: doi:10.1038/nchembio.2233

SUPPLEMENTARY RESULTS

Supplementary Table 1 – Mutant and wild type bioswitch performance

Variant	Fold Change	SEM (±)	T_{off}	T_{max}
TlpA	355	45	31.4	44.6
$TlpA_{36}$	370	63	31.4	44.6
$TlpA_{39}$	1523	434	31.4	44.6
TcI	1432	404	34.2	40
TcI_{38}	1032	160	32.4	40
TcI_{42}	1692	444	32.4	45.7

***** The reported T_{off} for each variant is the lowest temperature at which fluorescence could be detected above noise. T_{max} is the temperature at which fluorescence was maximal.

Supplementary Table 2 – Genetic constructs used in the study

All plasmids were constructed using the pETDuet-1 backbone (EMD Biosciences) with the relevant thermal biosensor elements replacing multiple cloning sites 1 and 2.

Plasmid	Transcriptional Regulator(s)	Output Gene Product(s)
pTlpA-Wasabi	TlpA	mWasabi
pTlpA-Wasabi-NF	TlpA	Nonfluorescent mWasabi (S71T, G73A)
pTcI-Wasabi	TcI (cI852 Repressor, cI A67T)	mWasabi
pLacI241-Wasabi	LacI A241T (mutation made in pETDuet-1 LacI)	mWasabi
pLacI265-Wasabi	LacI G265D (mutation made in pETDuet-1 LacI)	mWasabi
pTetR89-Wasabi	TetR A89D	mWasabi
pTetR193-Wasabi	TetR I193N	mWasabi
pLon-Wasasbi	Lon Promoter (GenBank CP009072)	mWasabi
pRpoH-Wasabi	RpoH Promoter (GenBank CP009072)	mWasabi
pClp-Wasabi	ClpP-ClpX Promoter (Genbank CP009072)	mWasabi
pHtpG-Wasabi	HtpG Promoter (Genbank CP009072)	mWasabi
pDnaK-Wasabi	DnaK Promoter (Genbank CP009072)	mWasabi
pGrpE-Wasabi	GrpE Promoter (Genbank CP009072)	mWasabi
pLacIq-Wasabi	LacIq Promoter	mWasabi
$pTlpA_{SP}$-Wasabi	TlpA Promoter with putative Pribnow box scrambled	mWasabi
$pTlpA_{Reverse}$-Wasabi	TlpA Promoter as reverse complement	mWasabi
$pTlpA_{36}$-Wasabi	$TlpA_{36}$	mWasabi
$pTlpA_{39}$-Wasabi	$TlpA_{39}$	mWasabi
$pTcI_{38}$-Wasabi	TcI_{38}	mWasabi
$pTcI_{42}$-Wasabi	TcI_{42}	mWasabi
pCali2	$TlpA_{36}$, TcI	mWasabi, mCherry
pThermeleon	TcI, TlpA, cI_{wt} (under control of TlpA)	mWasabi, mCherry
pKillswitch	$TlpA_{36}$	CcdA with SsrA degradation tag

Sources of genetic elements: TlpA: B. Finlay, Univ. British Columbia; mWasabi: F. Arnold, Caltech; mCherry: S. Qi, Stanford; CcdB: pLenti X1 Zeo DEST plasmid (Addgene #17299); TetR: pENTR1A plasmid (Addgene #22265); all other elements: Gblock synthesis (IDT).

Nature Chemical Biology: doi:10.1038/nchembio.2233

Supplementary Table 3 – List of mutations in selected variants of TlpA and TcI

Construct	Nonsynonymous Mutations	Synonymous Mutations
$TlpA_{36}$	P60L, D135V, K187R, K202I, L208Q	
$TlpA_{39}$	D135V, A217V, L236F	
TcI_{38}	M1V, L65S, K68R, F115L, D126G, D188G	A50 (GCT -> GCC), E128 (GAG -> GAA), R129 (AGA -> AGG), T152 (ACA -> ACC), L185 (CTT -> CTC)
TcI_{42}	K6N, S33T, Y61H, L119P, F122C	L51 (TTA -> CTA)

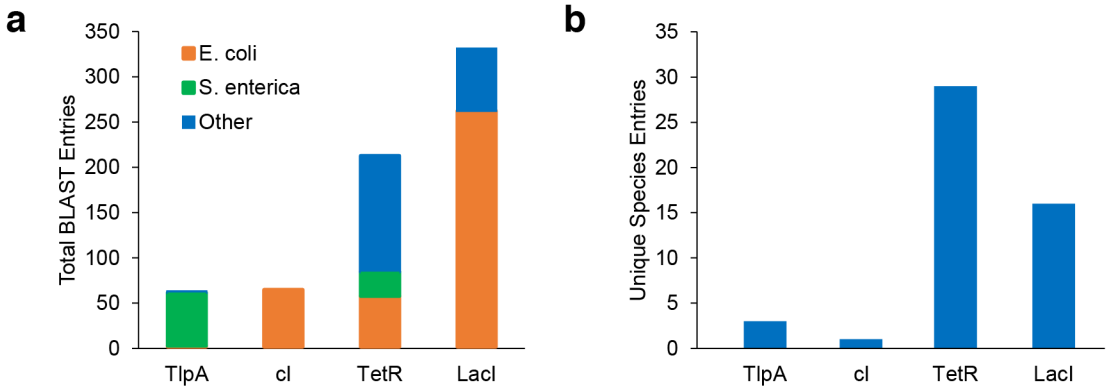

Supplementary Figure 1 – Prevalence of repressor sequences in bacteria. (a) National Center for Biotechnology Information (NCBI) Basic Local Alignment Search Tool (BLAST) search results for the wild type tlpA, cI, tetR, and lacI genes showing the cumulative number of hits obtained. The NCBI nucleotide collection was searched with the source organism restricted to bacteria. Cloning vectors, synthetic constructs, and individual gene sequences were omitted; genomic and naturally occurring plasmid sequences were retained. Sequences with alignment lengths of less than 90% of the wild type protein sequence were not included. The lacI gene is distributed throughout many commonly utilized *E. coli* strains such as Nissle 1917 and BL21, whereas the cI gene is found in less widely used *E. coli* strains. (b) The number of bacterial species in which the selected repressors are found. Data were obtained as in (a) and substrains were binned together. TlpA is largely restricted to *S. enterica* and cI to *E. coli*; tetR and lacI can be found in a larger number of bacterial species.

Nature Chemical Biology: doi:10.1038/nchembio.2233

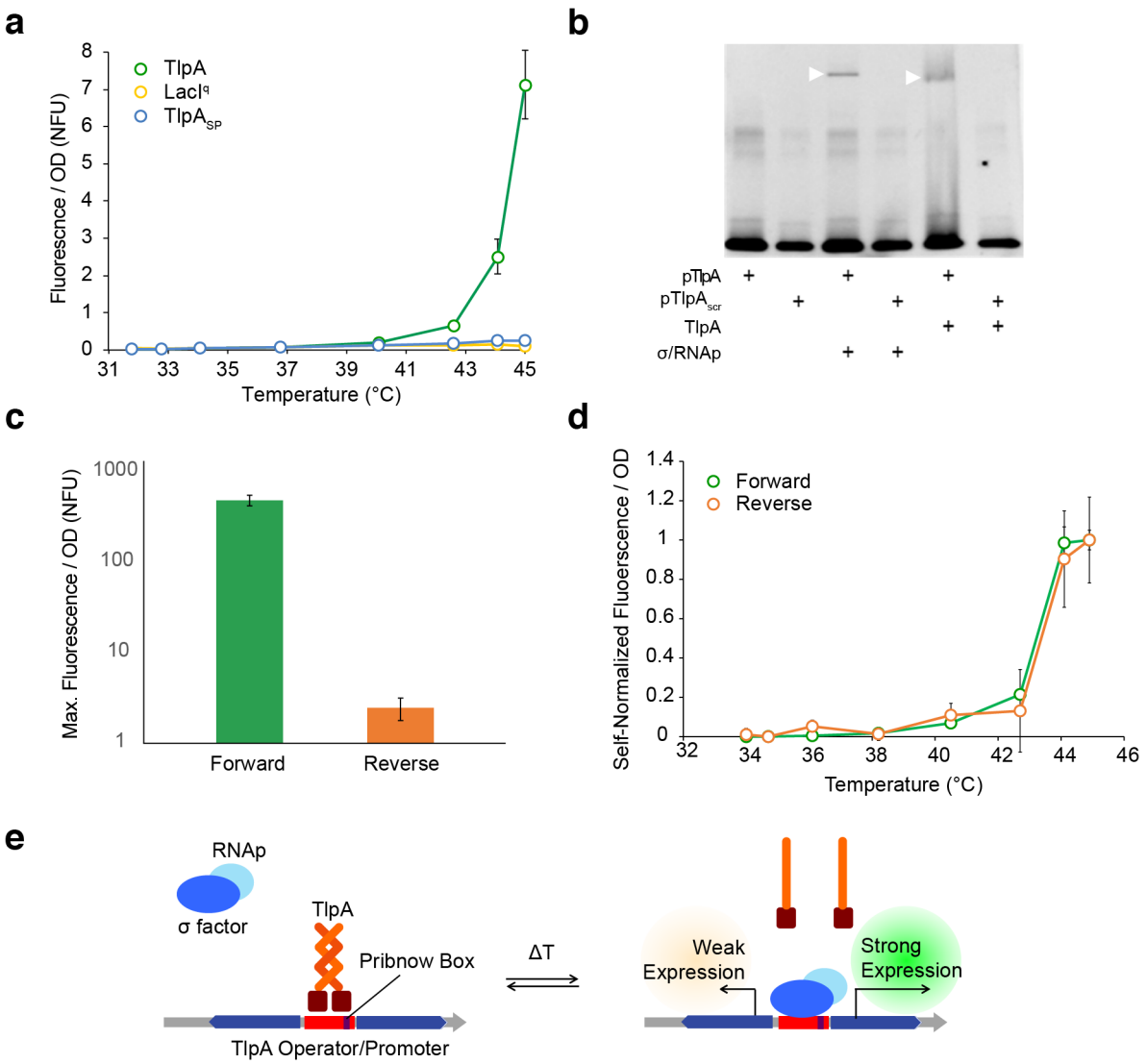

Supplementary Figure 2 – Mechanisms and bidirectional activity of the TlpA operator. (**a**) OD-normalized expression of the GFP reporter gene under the control of TlpA, LacI^{q}, and TlpA$_{SP}$ (in which nucleotides within the Pribnow box of the operator are shuffled). (**b**) Electromobility shift assay using a FAM-labeled TlpA operator oligonucleotide, demonstrating association of the operator with both TlpA and the *E. coli* σ^{70}-RNAp holoenzyme. In contrast, scrambled TlpA operator fails to associate with these proteins. The TlpA and σ^{70}-RNAp concentrations used in this experiment (1 μM and 0.18 μM, respectively) were similar to previous literature.[7,8] (**c**) GFP expression driven by the TlpA operator in the canonical and flipped orientations at 44.1°C. (**d**) Thermal induction profiles for GFP expression under the control of forward and reverse-oriented TlpA operator. Each curve is self-normalized to its maximal fluorescence intensity. (**e**) Proposed mechanism of TlpA-based thermal transcriptional regulation.

Nature Chemical Biology: doi:10.1038/nchembio.2233

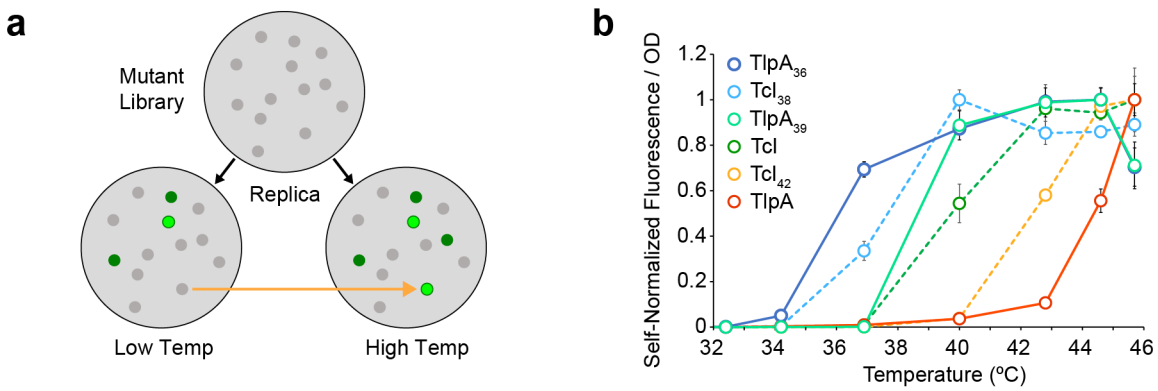

Supplementary Figure 3 - Tuning the transition temperature of thermal bioswitches. (**a**) Illustration of the screening strategy used to identify temperature-shifted repressor variants. (**b**) Self-normalized fluorescence/OD profiles for the full set of TlpA (solid lines) and TcI (dashed lines) bioswitches, demonstrating the complete range of available transition temperatures.

Nature Chemical Biology: doi:10.1038/nchembio.2233

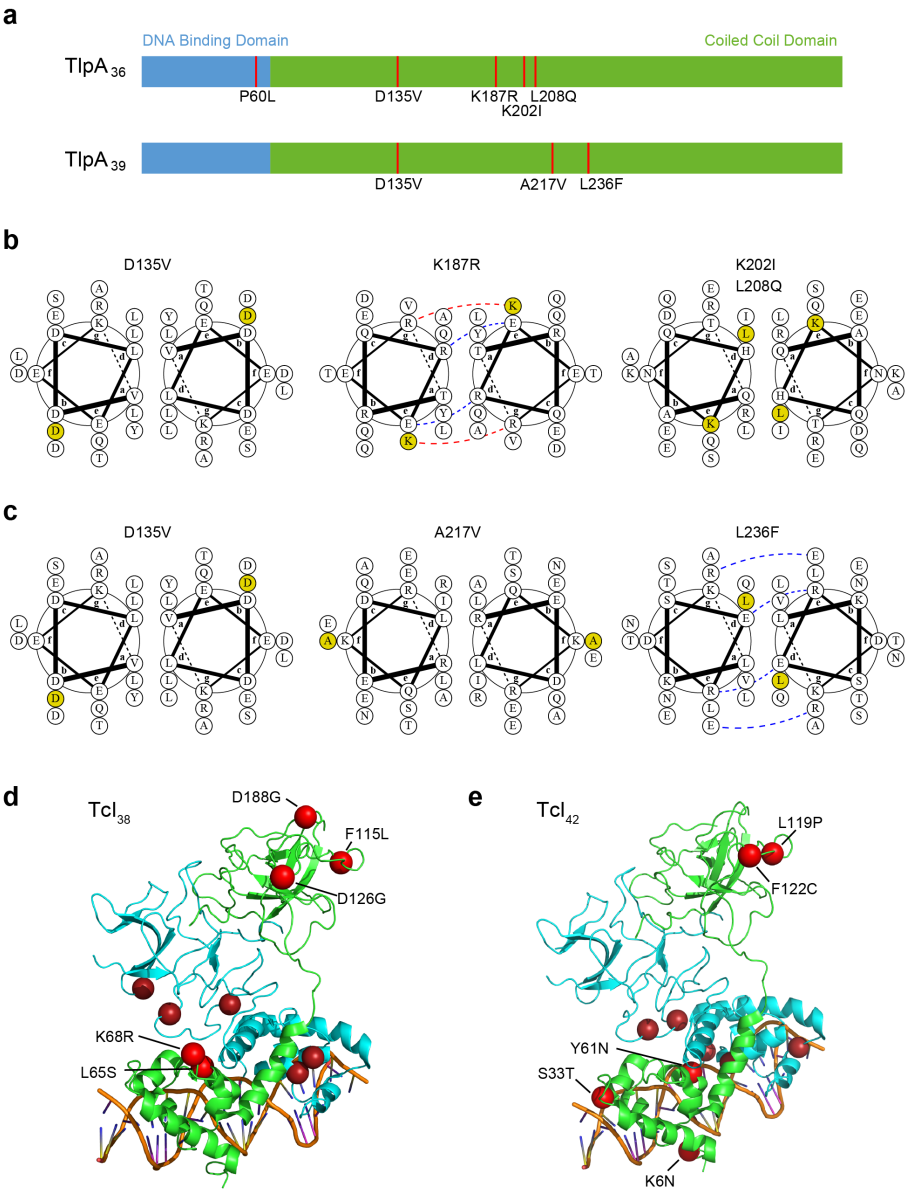

Supplementary Figure 4 – Positions of mutations in selected variants of TlpA and TcI. (**a**) Schematic of mutation positions (red) within the predicted domain structure of $TlpA_{36}$ and $TlpA_{39}$. The DNA binding domain is depicted in blue and coiled-coil domain in green, as delineated by Koski et al[1]. The figure is drawn to the scale of the primary sequence. (**b**) Positions of mutations in $TlpA_{36}$ within the predicted structure of the coiled-coil interface as viewed down the long axis of the helix. Blue dashed lines represent predicted energetically favorable ionic interactions; red dashes indicate predicted repulsive ionic interactions. The coil register was assigned based on consensus between previous literature[1] and the structure prediction servers COILS[2], Paircoil2[3], and LOGICOIL[4]. The images were produced using DrawCoil 1.0[5]. The P60L mutation is not shown because it falls outside of the predicted coiled-coil region. (**c**) Positions of mutations in $TlpA_{39}$. Register prediction and illustration were performed as in (b). (**d**) Mutation positions (red) for the lambda repressor variant TcI_{38}. The crystal structure of the wild type lambda repressor (PDB code 3BDN) was used as the homology model[6]. The original temperature-sensitizing mutation A67T is not shown. The M1V mutation is not depicted because residue 1 was not reported in the crystal structure. (**e**) Mutation positions (red) within the TcI_{42} variant.

Nature Chemical Biology: doi:10.1038/nchembio.2233

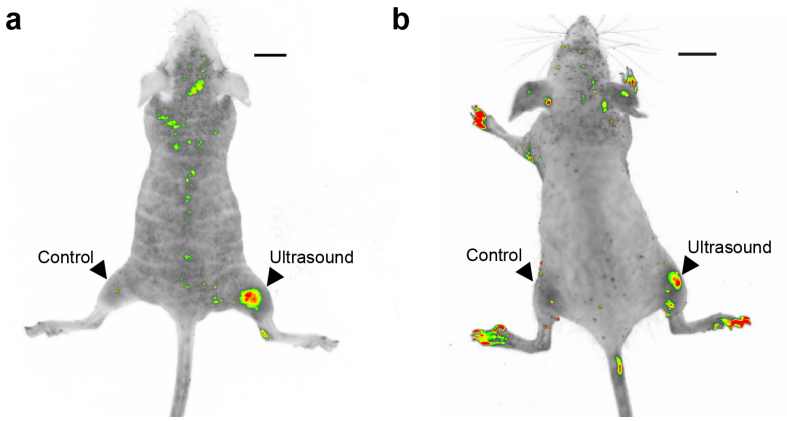

Supplementary Figure 5 – Additional mice with ultrasound-activated gene expression. (**a**) and (**b**) Additional mice that underwent the experiment shown in Fig. 4e. The images are thresholded fluorescence maps of mice injected subcutaneously in both left and right hindlimbs with *E. coli* expressing GFP under the control of $TlpA_{36}$, following ultrasound activation at only the right hindlimb. Signal at mouse digits is the result of autofluorescence and varies from mouse to mouse; digits were neither injected with bacteria nor exposed to ultrasound.

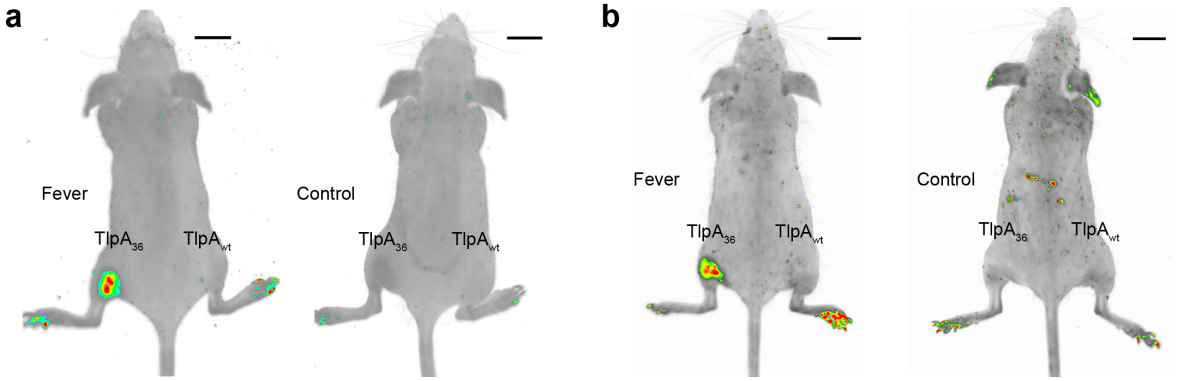

Supplementary Figure 6 – Additional mice with fever-activated gene expression. (**a**) and (**b**) Additional pairs of mice that underwent the experiment shown in Fig. 5, b-c. Each panel shows thresholded fluorescence maps of one mouse that underwent fever induction after being injected subcutaneously with plasmids expressing $TlpA_{36}$- and TlpA-regulated GFP into the left and right hind limbs, respectively, with a paired mouse that was prepared identically but maintained at room temperature.

Nature Chemical Biology: doi:10.1038/nchembio.2233

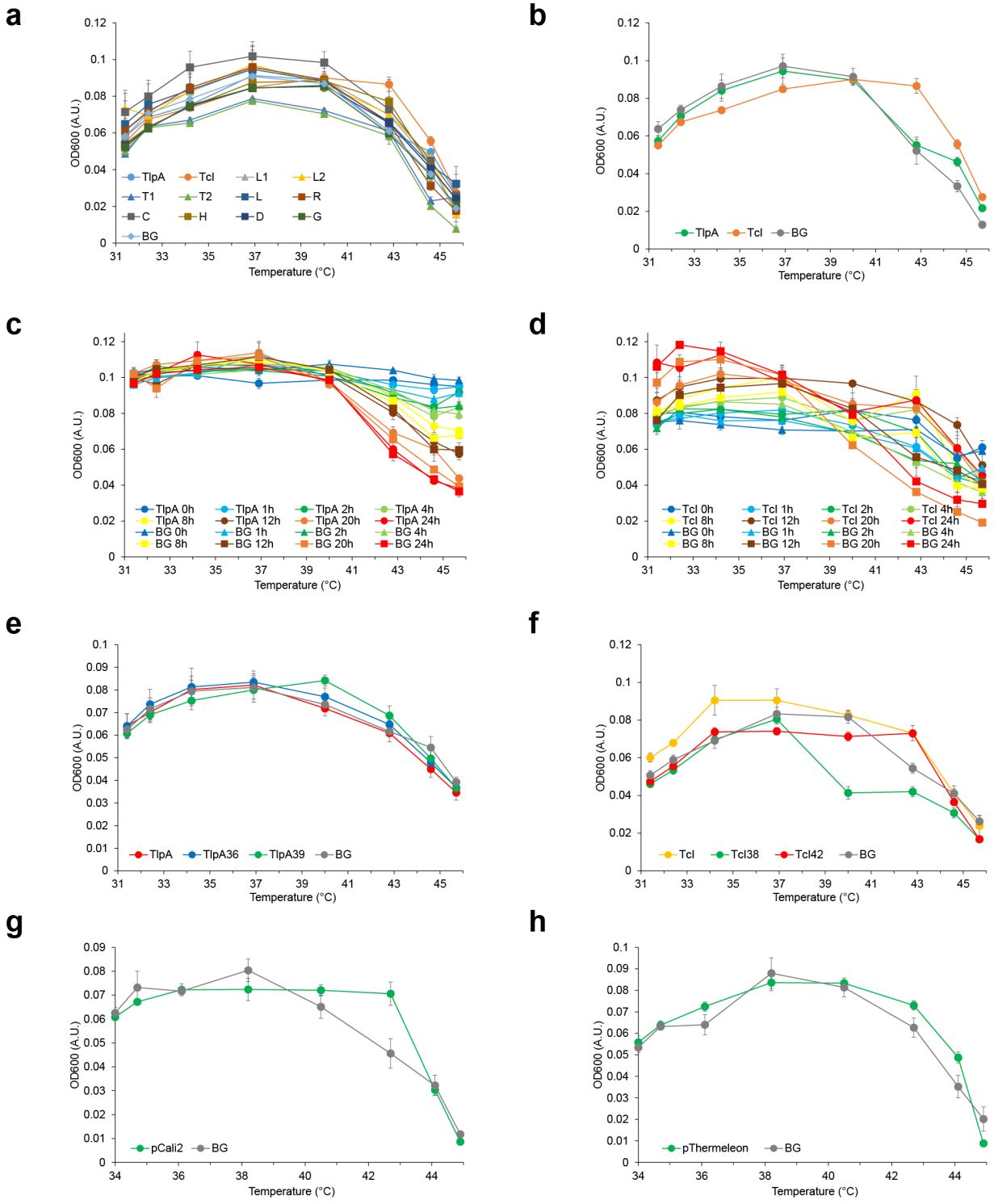

Supplementary Figure 7. OD_{600} measurements for thermal induction profiles reported in main text. Blank-subtracted measurements of OD_{600} in 90 µL volumes in clear-bottom 96 well plates, corresponding to an optical path length of approximately 1.4 mm. Data corresponds to: (**a**) Fig. 1b; (**b**) Fig. 1c; (**c**) Fig. 1e; (**d**) Fig. 1f; (**e**) Fig. 2d; (**f**) Fig. 2e; (**g**) Fig. 3c; (**h**) Fig. 3g. BG = background.

Nature Chemical Biology: doi:10.1038/nchembio.2233

Supplementary References

1. Koski, P., Saarilahti, H., Sukupolvi, S., Taira, S., Riikonen, P., Osterlund, K., … Rhen, M. A new alpha-helical coiled coil protein encoded by the Salmonella typhimurium virulence plasmid. *The Journal of Biological Chemistry* **267**, 12258–12265 (1992).
2. Lupas, A., Van Dyke, M., and Stock, J. Predicting Coiled Coils from Protein Sequences. *Science* **252**, 1162-1164 (1991).
3. McDonnel, A.V., Jiang, T., Keating, A.E., Berger B. Paircoil2: Improved prediction of coiled coils from sequence. *Bioinformatics* **22**, 356-358 (2006).
4. Vincent, T.L., Green, P.J., Woolfson, D.N. LOGICOIL—multi-state prediction of coiled-coil oligomeric state. *Bioinformatics* **29**, 69-76 (2013).
5. Grigoryan, G., Keating, A.E. Structural Specificity in Coiled-coil Interactions. *Current Opinion in Structural Biology* **18**, 477-483 (2008).
6. Stayrook. S.E., Jaru-Ampornpan, P., Ni, J., Hochschild, A., Lewis, M. Crystal structure of the lambda repressor and a model for pairwise cooperative operator binding. *Nature* **452**, 1022-1025 (2008).
7. Hurme, R., Berndt, K. D., Namork, E. & Rhen, M. DNA binding exerted by a bacterial gene regulator with an extensive coiled-coil domain. *The Journal of biological chemistry* **271**, 12626-12631 (1996).
8. Marr, M. T. & Roberts, J. W. Promoter Recognition As Measured by Binding of Polymerase to Nontemplate Strand Oligonucleotide. *Science* **276**, 1258-1260 (1997).

Nature Chemical Biology: doi:10.1038/nchembio.2233